Yield Stress and Elongation Prediction and Process Parameter Optimization of Two C-Mn Steels Based on XGBoost and Non-dominated Sorting Genetic Algorithm-II

Xu QIN, Xinqian ZHAO, Zhaoyang JIN, Qinghang WANG *

School of Mechanical Engineering, Yangzhou University, Yangzhou 225127, China

http://doi.org/10.5755/j02.ms.36556

Received 18 March 2024; accepted 11 April 2024

Mechanical properties are the key guidance for controlling the product quality of steel and optimizing its process. In this work, four machine learning (ML) algorithms (XGBoost, SVR, BP, and RBF) are used to establish a correlation model between chemical composition, process parameters, and mechanical properties for performance optimization. The ML model showing high prediction accuracy is selected to analyze the importance of the model parameters. The XGBoost model has the highest prediction accuracy, with both yield strength (YS) and elongation-to-failure (EL) achieving a prediction accuracy of over 0.9 on the testing set. Subsequently, the (YS) and (EL) of typical steel grades SPHC and Q235B are optimized by combining the high-precision XGBoost model and NSGA-II multi-objective optimization strategy. A comprehensive mechanical performance evaluation index (CP and EV) was proposed to screen the optimal Pareto frontiers, and two types of steel with excellent performance were successfully selected.
Keywords: C-Mn steel, machine learning, mechanical properties, XGBoost, NSGA-II.

1. INTRODUCTION

Steel is the most widely used structural engineering material in construction, automobile, ship, railroad, and other fields [1]. Mechanical properties are the key indicators of steel quality, and accurate prediction of the mechanical properties of products is of great significance in controlling product quality and optimizing product processes [2]. Since the production of hot rolled steel plate is a physical metallurgical process with a complex mechanism of action and a high degree of coupling of various factors, the prediction of mechanical properties is a complex, multidimensional, and nonlinear problem [3]. The traditional mechanism model and regression model are difficult to achieve accurate and reliable prediction, and they cannot adapt to the needs of actual industrial production.

Data-driven modeling [4] is one of the common techniques in the field of artificial intelligence, which mines the rules and patterns in the data through data mining, model fitting, and other methods, to predict the effects of different production process conditions on the mechanical properties of steel [5]. As a common data-driven technique, machine learning (ML) uses algorithms and statistical models to analyze and process data, thus adapting to the complexity and nonlinear relationships of the data [6]. Compared with traditional experimental research methods, it has more accurate and reliable data analysis and prediction capabilities. With these outstanding performances, it plays an important role in material property optimization and alloy design [7, 8].

In recent years, ML algorithms have received wide attention in the field of mechanical property prediction due to their intelligent and adaptable features [9]. Among different ML models, XGBoost (Extreme Gradient Boosting) is flexible, portable, efficient, and has won most of the ML competitions for structured data organized by the famous online Kaggle platform [10], but has not yet been seen to be used in the field of predicting the mechanical properties of carbon steels, where it can be combined with experimental methods in order to predict the physical properties of the material and to optimize the performance. For the design aspect of steel, a single mechanical property can no longer meet the design requirements of new steels [11], and the mechanical properties such as strength, ductility and toughness need to be considered together to achieve the best overall results [12]. Unfortunately, the two properties that need to be synergistically optimized are often contradictory [13], such as strength and ductility. The non-dominated sorting genetic algorithm-II (NSGA-II) is a progressive multi-objective evolutionary algorithm with an elite strategy [14], which uses the elite retention method for elitism to improve the adaptive fitting of the candidate solution population, and the combined application of ML and NSGA-II-makes the co-optimization of the mechanical properties of materials not difficult.

In this work, two mechanical properties, yield strength (YS) and elongation-to-failure (EL), and the XGBoost prediction model is combined with NSGA-II algorithm to predict and optimize the mechanical properties of steel. The experimental data of C-Mn steel are collected from the actual production data of a steel mill. By extracting and analyzing the key variables through the feature selection method, four ML mechanical property prediction models were established, and the best-performing prediction model was applied to the optimization of the composition and production process, it successfully predicted the

* Corresponding author. Tel.: +86-18883725047.
E-mail: *wangqinghang@yzu.edu.cn* (Q.H. Wang)

composition that maximized the comprehensive performance of C-Mn steel.

2. MATERIALS AND METHODS

The schematic flow of ML-based multi-objective optimization experimental design is shown in Fig. 1. First, Pearson correlation analysis was used to assess the relevance and importance of each input feature, and the production data were downscaled to remove redundant features [15]. Four ML methods, XGBoost, SVR (Support Vector Regression), BP (Backpropagation), and RBF (Radial Basis Function), were used to establish the mechanical performance prediction model. The prediction model with the highest accuracy was selected to evaluate the effect of the fluctuation of each input parameter on the mechanical properties by the control variable method. Finally, the NSGA-II was combined with the ML prediction model to optimize the chemical composition and processing of typical steel grades, define the comprehensive performance indexes, and prefer the Pareto front data to achieve the purpose of improving the comprehensive mechanical properties.

2.1. Data dimension reduction

The production data of several grades of carbon-manganese hot-rolled steel plates in a steel mill were used as the initial data samples, which had 19 dimensions, including 11 chemical compositions (C, Si, Mn, Ti, V, Al, S, Cr, P, Cu, and Ni) and 5 process parameters (RDT, FDT, CT, FDH, and LC) as inputs; 3 mechanical properties (YS, TS, and EL) as output targets. After data cleaning and preprocessing, 1000 sets of samples without residuals and obvious outliers were obtained.

Due to the large dimensionality of the data, Pearson correlation analysis was used to extract the input parameters that have a greater impact on the mechanical properties of carbon steel and to downscale the sample data. The Pearson correlation coefficient was used to measure the strength of the linear correlation between two fixed-distance variables X and Y and can be calculated as follows:

$$r_{xy} = \frac{(n\sum x_i y_i - \sum x_i \sum y_i)}{\sqrt{\left[n\sum x_i^2 - (\sum x_i)^2\right]\left[n\sum y_i^2 - (\sum y_i)^2\right]}}, \quad (1)$$

where n represents the sample size; x_i, y_i represent the values of the two variables; r_{xy} value is between (-1,1), the larger the absolute value, the stronger the correlation between the variables.

2.2. Model selection

In this work, four ML algorithms, BP, SVR, RBF and XGBoost, were used to establish a prediction model for the mechanical properties of hot rolled carbon steel, and the model with the best prediction accuracy and generalization ability was selected for carbon steel composition and process optimization.

When modeling the ML algorithms, the data set was first divided into mutually exclusive training, validation, and test sets using the leave-out method, with a data ratio of 6:2:2. Subsequently, the model was trained using the data from the training set to solve the model parameters. The data from the validation set was used to perform hyperparameter optimization to screen out the best-performing hyperparameter combinations. The accuracy of the model was evaluated in the training and validation sets, and the model's generalization ability was assessed in the test set to compare the accuracy and efficiency of the four ML algorithms. Evaluate the accuracy of the model on the training and validation sets were evaluated and the generalization of the model on the test set was to compare the accuracy and efficiency of the four ML algorithms. The root mean square error (RMSE) and the coefficient of determination (R^2) were used for solving the model parameters, optimizing the hyperparameters, and evaluating the model accuracy and generalization ability, which can be calculated as follows:

$$RMSE = \sqrt{\frac{1}{m}\sum_{i=1}^{m}(y_i - \hat{y}_i)^2}; \quad (2)$$

$$R^2 = 1 - \frac{\sum_{i=1}^{m}(y_i - \hat{y}_i)^2}{\sum_{i=1}^{m}(y_i - \bar{y}_i)^2}, \quad (3)$$

where m is the number of samples; y_i is the actual value; $\bar{y}_i$ is the average of the actual values; $\hat{y}_i$ is the predicted value.

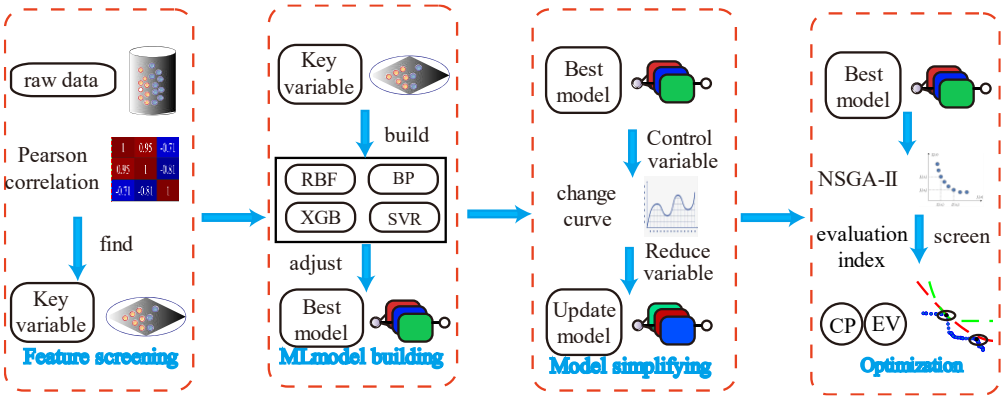

Fig. 1. Schematic diagram of multi-objective optimization experimental design process based on ML

2.3. NSGA-II multi-objective optimization

The NSGA-II multi-objective optimization algorithm avoids the loss of information and subjective preferences caused by the trade-offs between different objectives when transforming from a multi-objective to a single-objective problem. Moreover, it can find multiple Pareto optimal solutions and their corresponding Pareto front for the decision maker in a single run. The solutions in the Pareto frontiers are independent of each other, and each solution has its unique advantages and disadvantages, so that the decision maker can choose the most appropriate solution according to the actual needs and priorities. In addition, NSGA-II uses a fast non-dominated sorting algorithm and a congestion distance comparison operator to sort different individuals in the population.

The three elements of the optimization problem include decision variables, objective function, and constraints. The ML model with the highest prediction accuracy obtained in Section 3.2 is chosen to describe the quantitative relationship between the decision variables (chemical composition, hot rolling process) and the objective properties (YS and EL). For typical steel grades, such as SPHC and Q235B, the optimum values of chemical composition and hot rolling parameters are determined to maximize the YS and EL of steel plates when their values obey the constraint ranges of the industrial production data, expressed as follows:

$$obj: \begin{cases} \max\ \mathrm{YS}(X_i) \\ \max\ \mathrm{EL}(X_i) \end{cases}, \tag{4}$$

$$s.t: \min x_i < x_i < \max x_i, i = 1, 2, 3, \cdots, \mathrm{n}$$

where x_i denotes the decision variables screened out by the Pearson correlation coefficient, respectively; YS(x_i) and EL(x_i) are the YS and EL calculated by the aforementioned optimal ML model over the range of values of the decision variables.

Multi-objective optimization of chemical composition and process parameters of hot rolled steel plates based on NSGA-II was carried out in the following steps: 1) setting the chemical composition and hot rolling parameters of typical steel grades; 2) calculating the objective functions such as YS and EL by applying the optimal ML model obtained from the training of 2.2; 3) finding the Pareto-optimal solution of the problem variables in 1) by using the NSGA-II algorithm; 4) repeating the algorithm, obtaining the Pareto front by crossover and variational iteration; 5) analyzing the distribution characteristics of the Pareto optimal solution set and Pareto front to determine the optimal composition and process according to the actual demand.

It is well known that YS and EL are two conflicting performance metrics, and the optimized Pareto frontiers also exhibit a negative correlation but nonlinearity. In this study, to quantify the screening process of Pareto frontiers, two integrated mechanical property parameters CP (product of YS/MPa and EL/%) and EV (product of dimensionless YS_{norm} and EL_{norm} after normalization process) are defined, which can be calculated as:

$$YS_{norm} = \frac{YS - YS_{\min}}{YS_{\max} - YS_{\min}}, EL_{norm} = \frac{EL - EL_{\min}}{EL_{\max} - EL_{\min}}; \tag{5}$$

$$EV = YS_{norm} * EL_{norm}. \tag{6}$$

$$CP = YS * EL$$

3. RESULTS AND DISCUSSION

3.1. Data dimensionality reduction and analysis

The data are analyzed by calculating the Pearson correlation coefficient, as shown in Fig. 2.

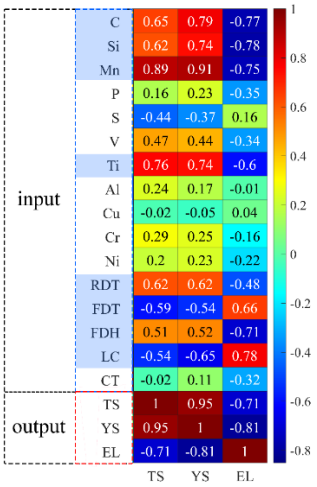

Fig. 2. Screening of Pearson correlation coefficient

The parameters with correlation coefficients less than 0.5 with the experimental parameters of mechanical properties are excluded, and a total of 8 parameters were retained as input parameters of the model, including 4 descriptors of the chemical composition of the material, which were C, Si, Mn and Ti; 4 descriptors of the processing conditions, which was RDT, FDT, LC and FDH. There are three descriptors for mechanical properties, namely YS, TS and EL. The values of all parameters in the dataset approximately obey the Gaussian distribution, as shown in Fig. 3.

3.2. Comparison of four different ML algorithms

Table 1 and Fig. 4 compare the prediction accuracy, running time and generalization ability of the four ML models. The RMSE of the XGBoost algorithm is higher than that of the BP, the RBF, and the SVR for both YS and EL. The reason may be because the XGBoost algorithm combines first-order and second-order derivatives for parameter optimization and incorporates a regular term to prevent overfitting, which improves the model performance. In the field of neural networks, the prediction accuracy of the RBF model is higher than that of BP, which may be related to the high dimensionality of the data in this work. The operational stability of the BP model is slightly higher than that of RBF, which may be related to the high dimensionality of the data. In addition, the XGBoost algorithm is characterized by fast training speed and high accuracy, and the model computation time is about 1.5 seconds, which is comparable to the SVR running time, and shorter than the 1.6 seconds of BP neural network and the 1.8 seconds of RBF neural network.

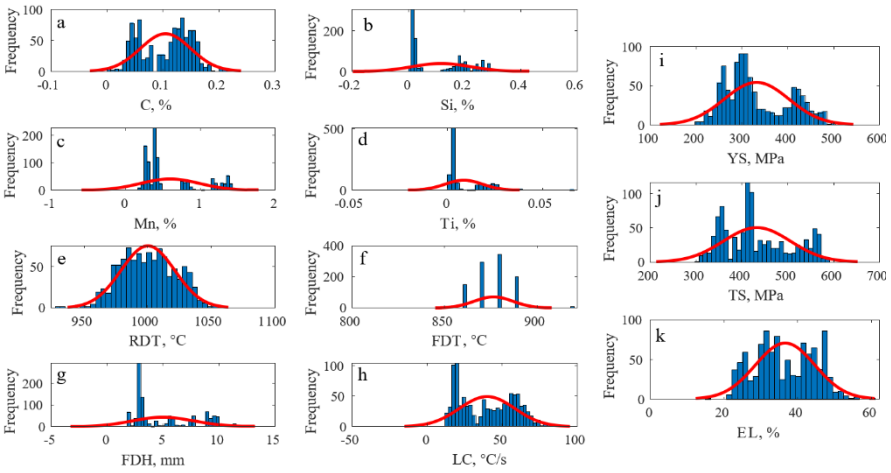

Fig. 3. Distribution of parameters in the dataset: a – C; b – Si ; c – Mn; d – Ti; e – RDT; f – FDT; g – LC; h – FDH; i – YS; j – TS; k – EL

Comprehensively comparing the prediction accuracy and computational efficiency of the four models, the XGBoost algorithm is more suitable for the prediction of mechanical properties of hot rolled steel, as well as the real-time control of the rolling process.

Table 1. Comparison of prediction accuracy and runtime of four ML models

ML	Data partition	Run time, s	RMSE
BP	Training set	1.6	13.6813
	Testing set		16.2411
RBF	Training set	1.8	16.0631
	Testing set		19.8457
XGBoost	Training set	1.5	6.4055
	Testing set		12.9750
SVR	Training set	1.6	17.1094
	Testing set		19.4490

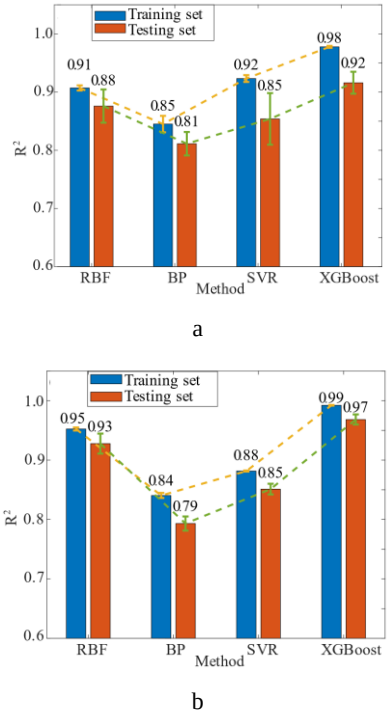

Fig. 4. Ten test runs for R^2 and variance to compare the generalization ability of four ML models: a – EL; b – YS

3.3. Influence of element content on mechanical properties

The correlation between C-Mn elemental content and mechanical properties is analyzed based on ML predictions, keeping the other influencing parameters at the average value [16]. Fig. 5 shows the predicted YS and EL at different elemental contents. YS changes insignificantly with increasing C, EL shows a decreasing trend, and decreases from 49.1 % to 36.7 %. Excessive C plays a weakening effect on ductility, which is in line with previous studies. Si has a beneficial effect on suppressing temper brittleness and improving temper resistance. With the increase of Si, the trend of YS and EL change is not obvious. The change of Mn changes the mechanical properties significantly. With the increase of Mn, EL shows a decreasing trend, EL decreases from 35.8 % to 27.7 %, and YS improves from 272 MPa to 441 MPa. The increase of Mn leads to a certain amount of Mn solid solution into the matrix organization, which results in the enhancement of the solid solution strengthening effect. Trace Ti also produces solid solution strengthening, but solid solution strengthening is not obvious. Continued addition of Ti presumably results in the formation of diffuse or precipitated phases. The formation of these phases can introduce dislocations in the crystal and impede the movement of the dislocations, resulting in a decreasing trend in EL.

At the same time, with the comparison of the addition of C and Mn, when the content of C increased from 0.05 to 0.15 wt.%, YS hardly changed with the change of C. When Mn is added from 0.3 to 1.2 wt.%, there is a significant change in YS. Although C is one of the main strengthening elements in steel and usually significantly improves its strength, the small changes in C have a relatively small impact on YS within the range of 0.05 – 0.15 wt.% C. This may be because the combined effect of solid solution strengthening and carbide precipitation strengthening do not show significant changes within the C range of 0.05 – 0.15 wt.%. With a significant increase in Mn, the solid solution strengthening effect is significantly enhanced, thereby significantly improving the YS of the steel. Therefore, within the given range of C, small changes in C have little effect on YS, while a significant increase in Mn

content can significantly improve the YS of C-Mn steel through solid solution strengthening and grain boundary strengthening mechanisms.

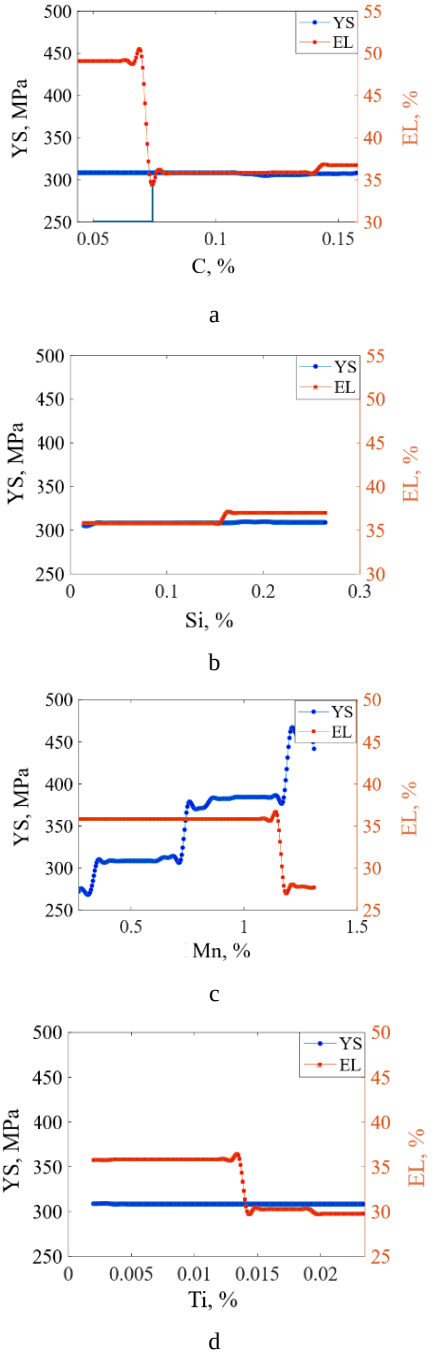

Fig. 5. Influence of element content on mechanical properties: a – C; b – Si; c – Mn; d – Ti

3.4. Optimization of input features using Pareto front combined with CP and EV

Taking SPHC and Q235B as an example, the NSGA-II multi-objective optimization method is used to optimize the composition and process of these two steel grades to achieve the synergistic enhancement of YS and EL. The range of values of the input variables of SPHC and Q235B is determined by the actual production data, as shown in Table 2. The Pareto optimal frontier obtained after solving the optimization model is shown as the blue solid circle in Fig. 6, the red hollow circle is the actual production data, and the red dashed line and green dotted line indicate the CP and EV indicator lines, respectively.

Table 2. Eight input parameters' ranges for Q235 and SPHC

Parameter	Q235B		SPHC	
	Minimum	Maximum	Minimum	Maximum
C, %	0.0618	0.1664	0.0022	0.0755
FDH, mm	1.98	11.54	2.58	3.80
Mn, %	0.344	1.061	0.194	0.322
RDT, °C	929.8	1035.3	931.0	1031.7
FDT, °C	860	890	870	920
LC, °C/s	12.9	44.4	36.7	84.1
Ti, %	0.001	0.008	0.001	0.066
Si, %	0.039	0.227	0.007	0.031

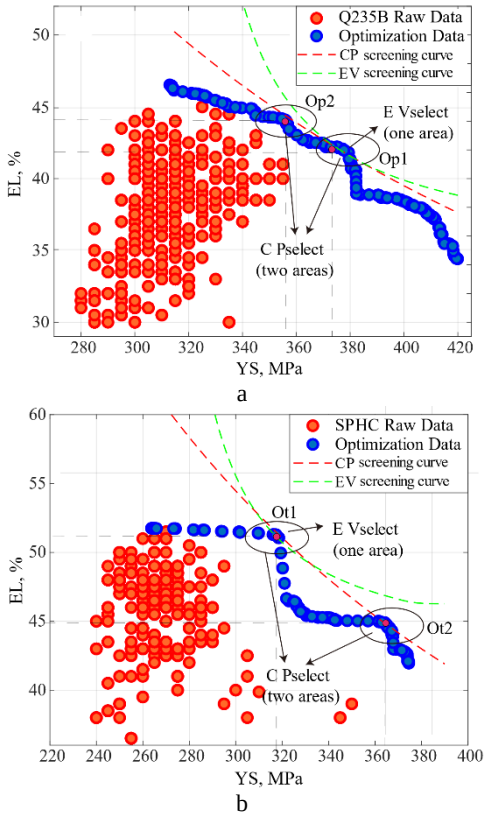

Fig. 6. SPHC and Q235B Pareto front Screening Results: a – SPHC steel; b – Q235B steel

From the Pareto optimal front in Fig. 5, it can be seen that the EL generally shows a decreasing trend with the increase of YS, i.e., the increase of YS is at the expense of the decrease of EL. For SPHC, when the YS is less than 320 MPa, the EL only slightly with the increase of YS, and once the YS exceeds 320 MPa, the increase of YS is accompanied by a sharp decrease of EL, and then the decrease tends to slow down; when the YS exceeds 360 MPa, the increase of its value is again accompanied by a sharp decrease of EL. The plotted CP index curves, which intersect the Pareto front and the optimum production data points, are at Ot1 and Ot2, respectively. Ot1 (YS about 318 MPa, EL about 51.2 %) and Ot2 (YS about 364 MPa, EL = 44.8 %). Similarly, for Q235B, Op1 (YS about 378 MPa, EL about 41.9 %) and Op2 (YS about 355 MPa, EL = 44.1 %) were obtained, with CP index values of 15838.2 and 15655.5, respectively, and the Pareto front for

Q235B showed a more uniform decreasing state, with only a small abrupt change in YS at 348 MPa, which is speculated to be related to the chemical composition, crystal structure and stability of the steel itself. The CP and EV screening results are calculated by XGBoost and NSGA-II algorithms as shown in Fig. 5. It can be found that the results screened by CP have two areas, while the results screened by EV have only one area. For Q235B, the chemical composition of the corresponding steel is $C_{0.062}$ $Si_{0.034}$ $Mn_{0.73}$ $Ti_{0.0016}$, where the numbers represent the constituents, which is the most promising largest CP and the promising largest EV. For SPHC steel grade, the chemical composition of the corresponding steel grade is $C_{0.024}$ $Si_{0.007}$ $Mn_{0.195}$ $Ti_{0.0012}$, which is the most promising largest EV and the most promising largest CP. Overall, the CP has a wider search range compared to the EV. It can effectively avoid the impact of attribute scaling on the overall performance after normalization and more easily to screen the chemical components that are desired for screening [17]. The two corresponding areas are suitable for applications with high plastic toughness requirements (products subjected to impact, alternating loads, and processed by plastic forming), and high strength requirements, respectively.

At the same time, the screened compositions of the two carbon steels were examined to be different from any of the original datasets, which need further experiments to verify. In our work, we use XGBoost and NSGA-II algorithms combined with two comprehensive mechanical property evaluation indexes, which can guide the next experimental design.

4. CONCLUSIONS

In this study, two comprehensive mechanical property evaluation indexes are established to predict and optimize the comprehensive mechanical properties of C-Mn. Based on the collected data, four ML models are successfully constructed, among which the XGBoost algorithm performs the best in predicting the mechanical properties both in terms of accuracy and stability. YS and EL are optimized, according to the NSGA-II multi-objective optimization strategy, and two indexes (CP and EV) are proposed for the evaluation of the comprehensive mechanical properties and optimization of the chemical compositions of high-strength and high-plasticity C-Mn steels. As mentioned above, the comprehensive combination of XGBoost and NSGA-II algorithms provides new ideas for material design and process optimization, and it also acts as an effective tool for the development of new materials.

Acknowledgments

This research was funded by the National Natural Science Foundation of China (No. 52204407), the Natural Science Foundation of Jiangsu Province (No. BK20220595), the China Postdoctoral Science Foundation (No. 2022M723689) and the Postgraduate Research & Practice Innovation Program of Jiangsu Province (No. SJCX23_1913).

REFERENCES

1. **Phaniraj, M.P., Behera, B.B., Lahiri, A.K.** Thermo-Mechanical Modeling of Two Phase Rolling and Microstructure Evolution in the Hot Strip Mill: Part-II. Microstructure Evolution *Journal of Materials Processing Technology* 178 2006: pp. 388 – 394. https://doi.org/10.1016/j.jmatprotec.2006.03.173
2. **Wang, L.T., Deng, C.H., Dong, M., Shi, L.F., Zhang, J.P.** Development of Continuous Casting Technology of Electrical Steel and New Products *Journal of Iron and Steel Research International* 19 2012: pp. 1 – 6. https://doi.org/10.1016/S1006-706X(12)60051-X
3. **Yan, X., Sui, Y., Zhou, H., Sun, W., Jiang, Y., Wang, Q.** Influence of the Mg Content on the Microstructure and Mechanical Properties of Al-xMg-2.0Si-0.6Mn Alloy *Journal of Materials Research and Technology* 23 2023: pp. 3880 – 3891. https://doi.org/10.1016/j.jmrt.2023.02.046
4. **Hwang, R.C., Chen, Y.J., Huang, H.C.** Artificial Intelligent Analyzer for Mechanical Properties of Rolled Steel Bar by Using Neural Networks *Expert Systems with Applications* 37 2010: pp. 3136 – 3139. https://doi.org/10.1016/j.eswa.2009.09.069
5. **Ge, M., Su, F., Zhao, Z., Su, D.** Deep Learning Analysis on Microscopic Imaging in Materials Science *Materials Today Nano* 11 2020: pp. 100087. https://doi.org/10.1016/j.mtnano.2020.100087
6. **Zhong, R., Salehi, C., Johnson, R.** Machine Learning for Drilling Applications: A Review *Journal of Natural Gas Science and Engineering* 108 2022: pp. 104807. https://doi.org/10.1016/j.jngse.2022.104807
7. **Bhattacharyya, T., Brat Singh, S., Sikdar, S., Bhattacharyya, S., Bleck, W., Bhattacharjee, D.** Microstructural Prediction Through Artificial Neural Network (ANN) for Development of Transformation Induced Plasticity (TRIP) Aided Steel *Materials Science and Engineering: A* 565 2013: pp. 148 – 157. https://doi.org/10.1016/j.msea.2012.11.110
8. **Golmohammadi, M., Aryanpour, M.** Analysis and Evaluation of Machine Learning Applications in Materials Design and Discovery *Materials Today Communications* 35 2023: pp. 105494. https://doi.org/10.1016/j.mtcomm.2023.105494
9. **Zhang, Y., Wen, C., Wang, C., Antonov, S., Xue, D., Bai, Y., Su, Y.** Phase Prediction in High Entropy Alloys with a Rational Selection of Materials Descriptors and Machine Learning Models *Acta Materialia* 185 2020: pp. 528 – 539. https://doi.org/10.1016/j.actamat.2019.11.067
10. **Yuan, Y., Du, J., Luo, J., Zhu, Y., Huang, Q., Zhang, M.** Discrimination of Missing Data Types in Metabolomics Data Based on Particle Swarm Optimization Algorithm and XGBoost Model *Scientific Reports* 14 2024: pp. 152. https://doi.org/10.1038/s41598-023-50646-8
11. **Pietrzyk, M., Kusiak, J., Kuziak, R., Madej, Ł., Szeliga, D., Gołąb, R.** Conventional and Multiscale Modeling of Microstructure Evolution During Laminar Cooling of DP Steel Strips *Metallurgical and Materials Transactions A* 45 2014: pp. 5835 – 5851. https://doi.org/10.1007/s11661-014-2393-z
12. **Zhao, L., Zhou, B., Zhu, W., Yan, C., Jin, Z., Guo, X.** A Comprehensive Study on the Mechanical Behavior, Deformation Mechanism and Texture Evolution of Mg Alloys with Multi Texture Components *Journal of Alloys and Compounds* 907 2022: pp. 164342. https://doi.org/10.1016/j.jallcom.2022.164342
13. **Ritchie, R.O.** The Conflicts Between Strength and Toughness *Nature Materials* 10 2011: pp. 817 – 822.

https://doi.org/10.1038/nmat3115

14. **Zhang, P., Qian, Y., Qian, Q.**, Multi-Objective Optimization for Materials Design with Improved NSGA-II *Materials Today Communications* 28 2021:102709. https://doi.org/10.1016/j.mtcomm.2021.102709
15. **Sensuse, D.I., Cahyaningsih, E., Wibowo, W.C.** Identifying Knowledge Management Process of Indonesian Government Human Capital Management Using Analytical Hierarchy Process and Pearson Correlation Analysis *Procedia Computer Science* 72 2015: pp. 233 – 243. https://doi.org/10.1016/j.procs.2015.12.136
16. **Zhang, Y., Bai, S., Jiang, B., Li, K., Dong, Z., Pan, F.** Modeling the Correlation Between Texture Characteristics and Tensile Properties of AZ31 Magnesium Alloy Based on the Artificial Neural Networks *Journal of Materials Research and Technology* 24 2023: pp. 5286 – 5297. https://doi.org/10.1016/j.jmrt.2023.04.079
17. **Diao, Y., Yan, L., Gao, K.** A Strategy Assisted Machine Learning to Process Multi-Objective Optimization for Improving Mechanical Properties of Carbon Steels *Journal of Materials Science & Technology* 109 2022: pp. 86 – 93. https://doi.org/10.1016/j.jmst.2021.09.004